Cancer Research

JPO2/CDCA7L and LEDGF/p75 Are Novel Mediators of PI3K/AKT Signaling and Aggressive Phenotypes in Medulloblastoma

Tiffany Sin Yu Chan[1,2], Cynthia Hawkins[2,3], Jonathan R. Krieger[2], C. Jane McGlade[2,4], and Annie Huang[1,2]

Abstract

Substantial evidence links Myc–PI3K/AKT signaling to the most aggressive subtype of medulloblastoma and this axis in medulloblastoma therapy. In this study, we advance understanding of how Myc–PI3K/AKT signaling contributes to this malignancy, specifically, in identifying the Myc-interacting protein JPO2 and its partner binding protein LEDGF/p75 as critical modulators of PI3K/AKT signaling and metastasis in medulloblastoma. JPO2 overexpression induced metastatic medulloblastoma *in vivo* through two synergistic feed-forward regulatory circuits involving LEDGF/p75 and AKT that promote metastatic phenotypes in this setting. Overall, our findings highlight two novel prometastatic loci in medulloblastoma and point to the JPO2:LEDGF/p75 protein complex as a potentially new targetable component of PI3K/AKT signaling in medulloblastoma. *Cancer Res; 76(9); 2802–12. ©2016 AACR.*

Introduction

Medulloblastoma, a primitive neuroectodermal tumor of the cerebellum, is the most common malignant pediatric brain tumor (1). Despite recent advances in clinical risk stratification and intensified therapies, approximately one-third of children with medulloblastoma will succumb to their disease. Metastasis, which is found in 30% to 40% of patients at diagnosis, is one of the strongest predictors of survival. However, current approaches for controlling or preventing metastases are often ineffective and frequently leave survivors with severe long-term toxicity (2).

Recent genomic studies indicate four molecular subgroups of medulloblastoma (3) and confirmed early observations of the strong negative prognostic effect of *MYCC* amplification, which defines the most aggressive group 3 medulloblastoma (3–5). Our studies and those of others have shown that Myc can confer metastatic phenotypes in medulloblastoma (6–8). Although mechanisms of Myc-mediated transformation in medulloblastoma remain largely unknown, multiple lines of data suggest Myc-driven medulloblastoma are dependent on PI3K/AKT signaling (6–16) and point to the PI3K/AKT axis as a critical downstream effector of Myc in group 3 medulloblastoma (7, 16, 17). Activation of PI3K/AKT signaling has been shown to promote various oncogenic phenotypes in medulloblastoma including enhanced tumor growth, metastasis, and chemoresistance (14, 18–22). Thus, defining the scope of Myc regulatory network in medulloblastoma will clearly be important for informing more effective targeting of the Myc–PI3K/AKT axis.

In prior work, we discovered a Myc cotransforming protein partner—JPO2 (CDCA7L/RAM2/R1; ref. 23), which acts synergistically with Myc in transcriptional repression (6) and is upregulated in metastatic medulloblastoma (23, 24). Although these observations suggested important functional roles for JPO2 in medulloblastoma oncogenesis (25, 26), the specific role of JPO2 in medulloblastoma transformation remains unknown.

In this study, we demonstrate that JPO2 like Myc, potently and directly induces metastatic and infiltrative medulloblastoma in orthotopic models. We identify LEDGF/p75 as a binding partner of JPO2 in medulloblastoma, and show that JPO2 acts cooperatively with LEDGF/p75 to promote medulloblastoma cell migration via a novel feed-forward regulatory circuit that converges on AKT signaling. Our studies underscore AKT as a critical prometastatic signaling pathway in medulloblastoma and reveal JPO2 and LEDGF/p75 as novel therapeutic targets in AKT signaling.

Materials and Methods

Cell culture

Medulloblastoma cell lines D283, D341, D458 [gifts from Dr. Bigner (2003), Duke University (Durham, NC)] were maintained in zinc option medium (Life Technologies); UW228, UW426 [gifts from Dr. Silber (2003), University of Washington (Seattle, WA)), and DAOY (ATCC, 2005) were maintained in αMEM containing 10% FBS. 293T cells were maintained in DMEM (Life Technologies) with 10% FBS. For transient expression, 293TV

[1]Department of Paediatrics, Laboratory Medicine and Pathobiology, University of Toronto, Toronto, Ontario, Canada. [2]Arthur and Sonia Labatt Brain Tumor Research Centre, The Hospital for Sick Children, Toronto, Ontario, Canada. [3]Department of Pathology, The Hospital for Sick Children, Toronto, Ontario, Canada. [4]Department of Medical Biophysics, University of Toronto, Toronto, Ontario, Canada.

Note: Supplementary data for this article are available at Cancer Research Online (http://cancerres.aacrjournals.org/).

Corresponding Author: Annie Huang, The Hospital for Sick Children, 555 University Avenue, Toronto, Ontario M5G 1 × 8, Canada. Phone: 416-813-7360; Fax: 416-813-8024; E-mail: annie.huang@sickkids.ca

doi: 10.1158/0008-5472.CAN-15-2194

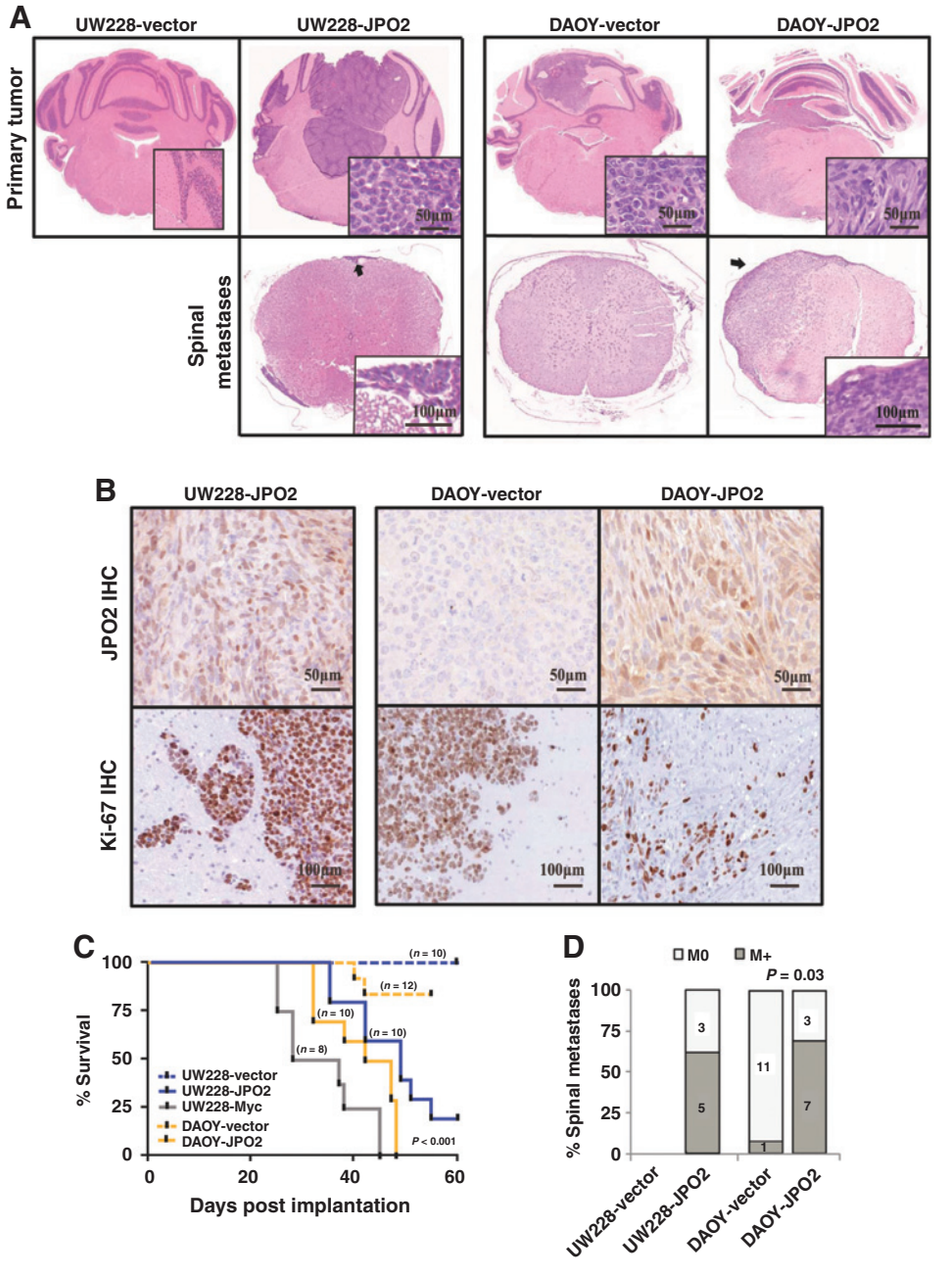

Figure 1.
JPO2 induces metastatic and infiltrative medulloblastoma tumor growth *in vivo*. Log-phase UW228 and DAOY cells (1×10^5) were orthotopically injected into cerebella of 5- to 6-week-old *Nu/Nu* mice, which were followed till death and brain and spine were removed for histopathologic studies. A, H&E stains of whole brain and spine from mice injected with UW228-JPO2, DAOY-JPO2, and corresponding control lines. Inset shows higher magnification images, and arrows indicate spinal metastases. B, tumor xenografts stained with anti-JPO2 or Ki-67 antibodies. C, Kaplan–Meier survival analyses of mice injected with UW228-JPO2, UW228-Myc, and DAOY-JPO2 and corresponding control lines. D, frequency of spinal metastases in mice injected with control or JPO2-expressing UW228 and DAOY cell lines. Metastatic (M+) and nonmetastatic tumors (M0) were determined by histologic examination of the entire spinal cord. Number of mice with M0 and M+ tumors are indicated.

cells were routinely transfected with 2 to 5 μg of plasmids using Fugene (Roche Applied Science) at a 3:1 ratio of Fugene/plasmid DNA and analyzed by RT-PCR and Western blotting 24 to 48 hours later.

To generate stable JPO2/LEDGF-expressing cell lines, cells were infected with pMN-GFP-JPO2/eGIPz-RFP-LEDGF or corresponding vector control. FACS-enriched cells were expanded and protein expression verified by Western blotting, as described previously (27). Stable expressions were tested each time when cells were grown from frozen stock prior to experiments.

For generating sh-JPO2–stable expressing cell lines, *JPO2* RNAi construct as described previously: forward, 5′-CCGG-AATGGTCGTGGAGTCAGATT TCAAGAGAATCTGACTCCAC-GACCATTTTTTTG-3′; and reverse, 5′-AATTGGAGTCAGATT-CTCTTGAAATCTGACTCCACGACCATT-3′, were subcloned into psi-RNAi-plasmid with Zeocin selective marker. Cells were transfected with Fugene, selected with Zeocin, and tested for JPO2 expression by RT-PCR and Western blotting.

For RT-PCR, JPO2 primers (forward, 5′-GCGGAAGAGTTTTA-CAGC-3′; reverse, 5′-CTGACATCCTCCCCATAG-3′), LEDGF primers (forward, 5′-CACACAGAGATGATTACTACACTG-3′; reverse, 5′-CCATCTTGAGCATCAGATCCTC-3′), and previously described 36B4 primers were used (6).

Cell proliferation, death, and migration assays

Cell proliferation was assessed using MTS assays (Roche Colorimetric Cell Proliferation, Roche Pharmaceuticals) at regular

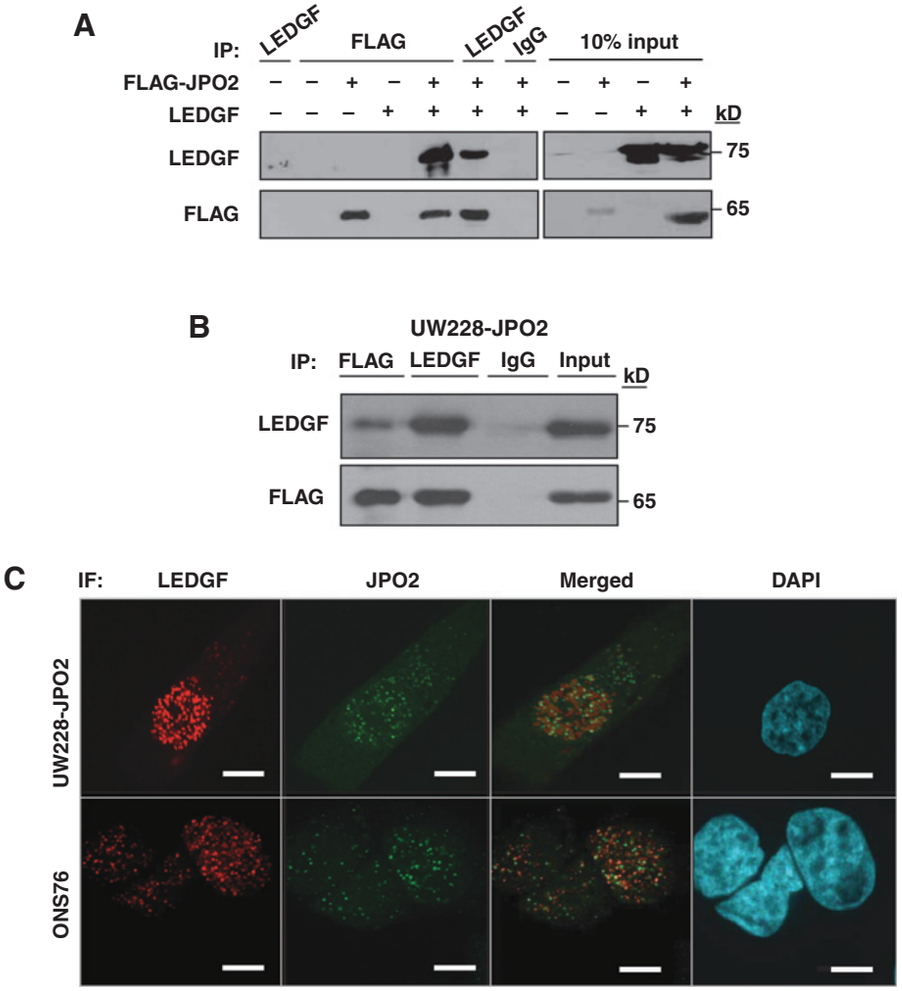

Figure 2.
JPO2 interacts with LEDGF/p75 in medulloblastoma cells. Nuclear lysates from 293 TV cells transiently transfected with CMV10-FLAG JPO2 or pGIPZ-LEDGF (A) and from UW228-JPO2 (B) were immunoprecipitated with anti-LEDGF or anti-FLAG antibodies. Coimmunoprecipitation of JPO2 or LEDGF and efficiency of immunoprecipitation were confirmed by Western blot analysis with anti-LEDGF (top) and anti-FLAG antibodies (bottom); 10% input controls is shown in last lane.
C, coimmunofluorescence studies of JPO2 and LEDGF/p75. UW228-JPO2 and ONS76 cells were fixed and stained with anti-LEDGF, anti-JPO2 antibodies, and DAPI. Colocalization of LEDGF (Alexa Fluor-568) and JPO2 (Alexa Fluor-488) was determined by confocal imaging. Scale bar, 20 μm.

intervals as described previously (6) and results were verified by direct Trypan blue cell count.

Bromodeoxyuridine (BrdUrd) assay was performed using the Cell Proliferation BrdUrd Chemiluminescent ELISA (Roche Pharmaceuticals). Briefly, cells were fixed and stained with anti-5-bromodeoxyuridine-POD antibody. Immune complexes and reactions were quantified using a multiwell luminometer.

Cell migration assays were performed as described previously (6) using Transwell Boyden chambers according to the manufacturer's instructions (BD Biosciences). In brief, 3.5×10^4 cells were seeded in chambers at 37°C for 18 to 40 hours. To quantify migrated cells, membranes were stained with 1% toluidine, migrated cell counts were determined on the basis of 10 random microscopic fields, counted by two individuals in a blinded fashion.

Orthotopic xenograft assays

Nu-Nu mice (Charles River Laboratories) were maintained in accordance with the Hospital for Sick Children Institutional Animal Care Committee–approved protocols. Briefly, cerebella of 4- to 6-week-old anesthetized male mice were injected stereotactically (guided coordinates $X = -2.0, Y = 2.0, Z = 2.0$) with 1×10^5 UW228/DAOY cells stably expressing JPO2. Specifically, a total volume of 1.5 μL was injected over 3 to 4 minutes. All animals were monitored for posterior fossa tumor-related symptoms such as hunched posture, doomed head, ataxia, weight loss and euthanized as per standard tumor endpoint monitoring guidelines. Dr. Cynthia Hawkins performed histopathologic analyses of whole brain and spine from all mice.

Histology and IHC

IHC was performed on formalin-fixed paraffin-embedded tissue using standard procedures. Xenograft specimen tissues were subjected to antigen retrieval by pressure cooking (citrate buffer, pH 6, 20 minutes) and 0.3% H_2O_2 endogenous peroxidase blocking. Primary antibody: JPO2 antibody [1:500, rabbit, in-house (6, 22)], Ki-67 (1:150; Dako, Agilent Technologies), were incubated overnight at 4°C and detected using biotinylated secondary IgG antibodies for 30 minutes using ABC Reagent Kit and DAB Chromagen (Vector Laboratories). A final counterstain was performed in hematoxylin followed by dehydration in 70%, 80%, and 100% ethanol series to xylene and mounted in Permount (Thermo Fisher Scientific). Hematoxylin and eosin (H&E) stains were performed using standard protocols.

Western blot and RNA analyses

Cell lines were lysed with standard EBC whole cell lysis buffer (50 mM Tris-HCl, 120 mM NaCl, 0.5% NP-40, and 5 mM EDTA, pH 8.0) as described previously (23), and analyzed by Western

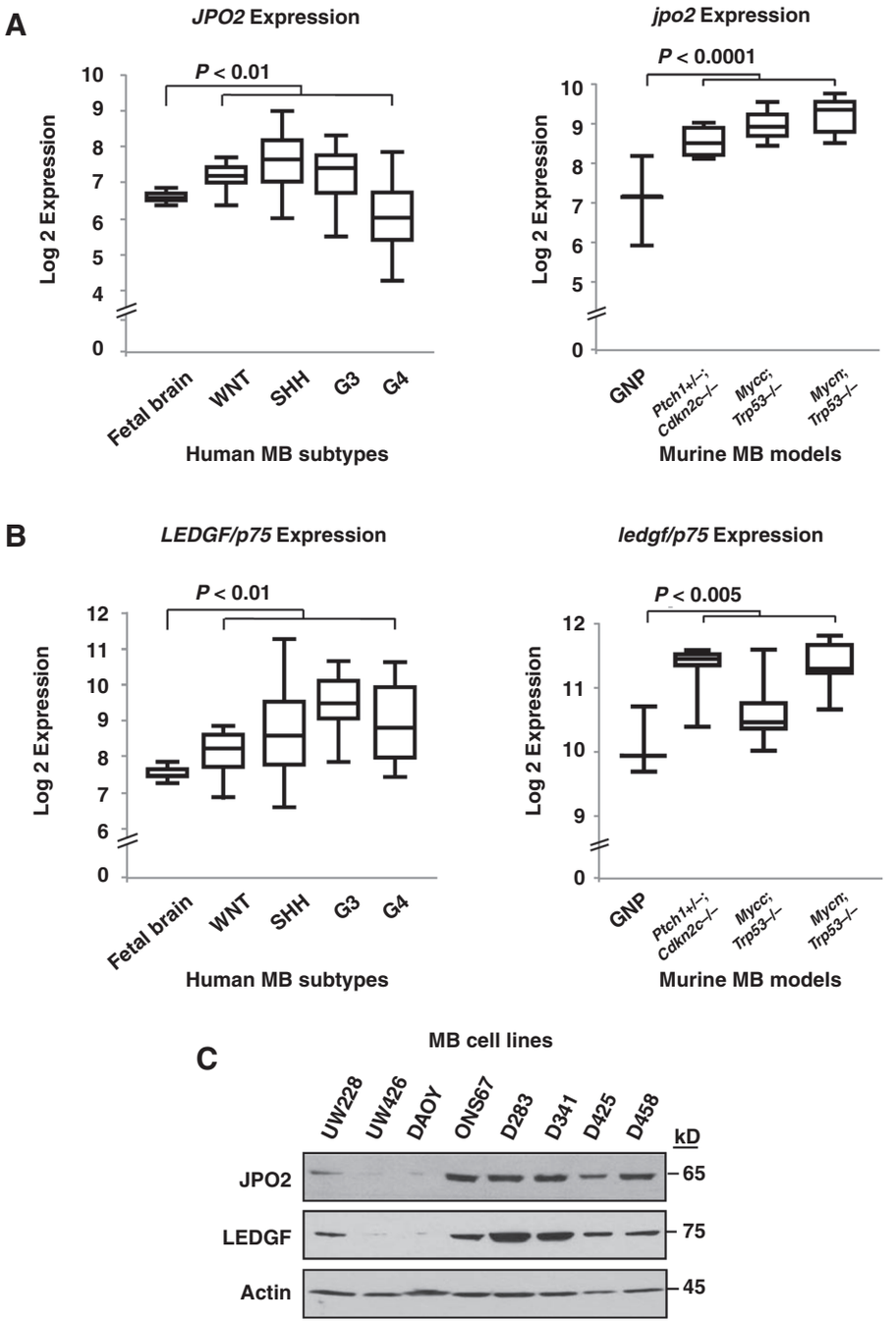

Figure 3.
JPO2 and LEDGF/p75 are concordantly upregulated in human and murine medulloblastoma, and medulloblastoma cell lines. *In silico* analyses of gene expression patterns for *JPO2/jpo2* (A) and *LEDGF/p75/ledgf/p75* (B) in primary human medulloblastoma (WNT, $n = 9$; SHH, $n = 34$; group 3, $n = 26$; group 4, $n = 34$), relative to fetal brain $n = 9$ (GSE10327) and murine medulloblastoma (right; *Ptch1+/-;cdkn2-/-*, $n = 7$; *Mycc*, $n = 14$; *Mycn*, $n = 10$) relative to granular neuron precursor cells (GNP, $n = 3$; GSE33201). C, Western blot analysis of JPO2 and LEDGF/p75 in a panel of medulloblastoma cell lines, with actin as loading control.

blotting with anti-JPO2 (1:500, rabbit, in-house; refs. 6, 23), Myc (1:500, in-house 9E10 mouse monoclonal; refs. 6, 23), α-tubulin (1:5,000; mouse, T9026; Sigma-Aldrich), LEDGF (1:1,000, mouse, MABN674; EMD Millipore), PARP (1:1,000, rabbit, 9542; Cell Signaling Technology), p-AKT308 (1:1,000, rabbit, 2965; Cell Signaling Technology), pan-AKT (1:1,000, rabbit, 2920; Cell Signaling Technology), pRAC/CDC424 (1:1,000, rabbit, 2461; Cell Signaling Technology), RAC1-3 (1:1,000, rabbit, 2456; Cell Signaling Technology), CDC42 (1:1,000, rabbit, 2464; Cell Signaling Technology), pThr202/Tyr204ERK1/2 (1:1,000, rabbit, 9101; Cell Signaling Technology), and ERK1/2 (1:1,000, rabbit 9102; Cell Signaling Technology). Detection was performed using antispecies horseradish peroxidase–conjugated antibodies (Bio-Rad Laboratories) and Chemiluminescence Reagent Plus (PerkinElmer).

RNA and cDNA were generated using standard methods for quantitative PCR analysis (SYBR Green PCR Kit, Invitrogen, Life Technologies; ABI Prism 7900HT Sequence Detection Systems, Applied Biosystems). Specific mRNAs were quantified relative to *36B4* using the $\Delta\Delta C_t$ method.

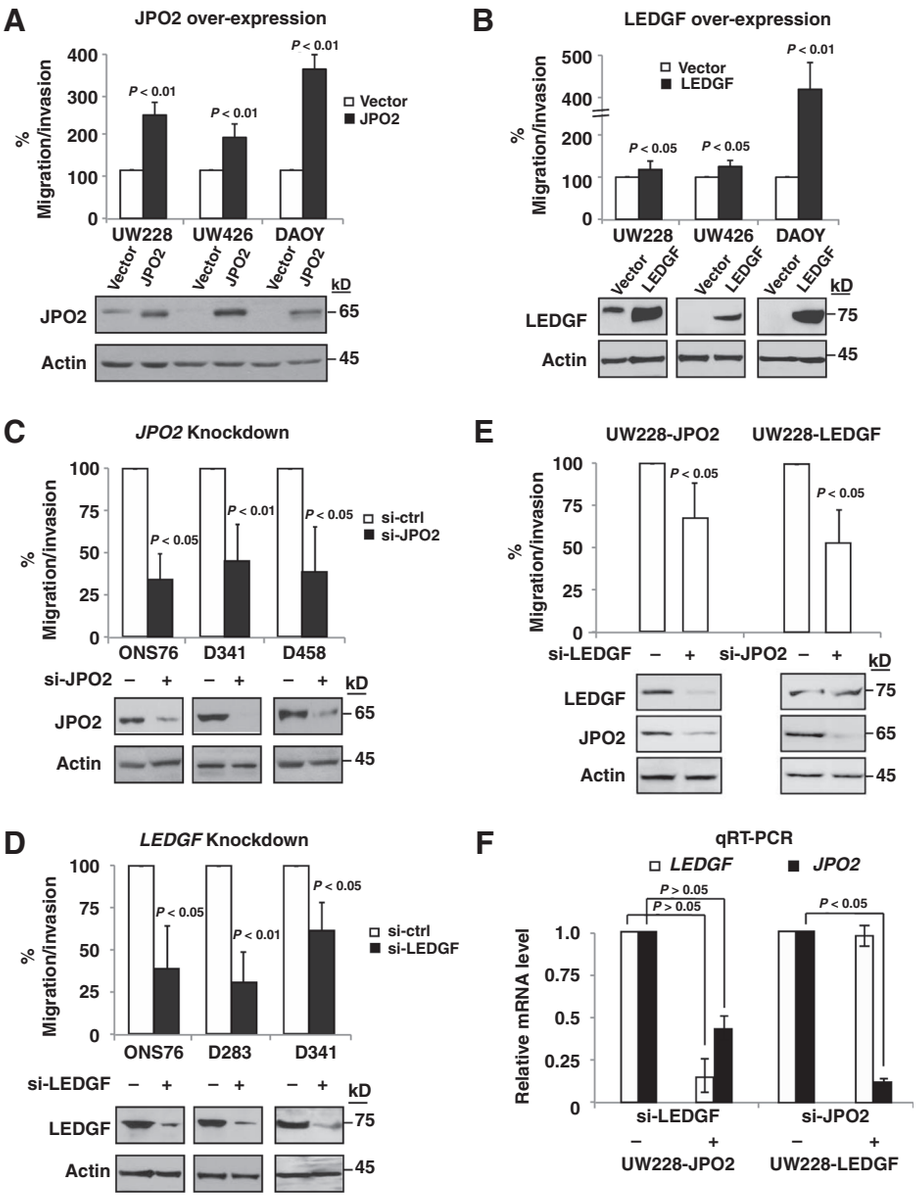

Figure 4.
JPO2 and LEDGF/p75 specifically promote medulloblastoma cell migration/invasion. UW228, UW426, and DAOY cells with stable JPO2 or LEDGF/p75 expression, or siRNA-mediated JPO2 or LEDGF/p75 knockdown for 24 hours and corresponding controls were seeded (3.5×10^4 cells) in Boyden chambers and migrated cells were determined by direct cell count after 22 to 48 hours. A—D, percent cell migration determined relative to controls is summarized for $n = 3$ experiments with 2 replicas/data point and is shown with corresponding Western blots for JPO2 or LEDGF/p75 with actin as loading control. Error bars, SEM; *, $P < 0.05$; **, $P < 0.01$ (range of migrated cell count = 50–200/field.). E, UW228 cells with stable JPO2 or LEDGF/p75 expression were, respectively, transfected with si-LEDGF/or si-JPO2 for 24 hours, and analyzed for cell migration as described above. Western blot analysis shows confirmation of JPO2 or LEDGF knockdown; actin served as loading control. F, corresponding qRT-PCR analysis of LEDGF/p75 and JPO2 expression. Data are presented as $2^{-\Delta\Delta C_t}$ (2 replicas/experiment, error bars, SE).

Mass spectrometry

Lysates of UW228-FLAG-JPO2 and UW228-FLAG-vector cells extracted in lysis buffer (50 mmol/L Tris pH 7.4, 150 mmol/L NaCl, 1 mmol/L EDTA, and 0.5% Triton X-100) were subjected to immunoprecipitation using anti-FLAG M2 beads (A2220, Sigma-Aldrich) for 3 hours, followed by washes in lysis buffer (1% NP-40 and 0.1% Triton X-100) and wash buffer. Subsequently, beads were washed with 20 mmol/L Tris buffer (pH 8.0), and eluted proteins were analyzed by SDS–PAGE and silver staining. Protein bands excised from gels were digested with trypsin, and resulting peptides were identified by LC/MS-MS sequencing. Specific JPO2-interacting proteins were identified on the basis of (i) peptides originating from UW228-JPO2 samples that were absent in UW228-vector control; (ii) proteins yielding more than two unambiguous peptides and appearing in two or more independent experiments.

Informatics and statistical analysis

Publicly available gene expression data for a series of human primary medulloblastoma samples (GSE10327; ref. 28) and mouse medulloblastoma samples (GSE33201; ref. 11) performed on Affymetrix U133 platforms were downloaded from the Gene Expression Omnibus (GEO) repository, and CEL files were integrated and analyzed using the Partek Genomics Suite (Partek). Transcript levels of *CDCA7L/JPO2* and *PSIP1/LEDGF* were investigated for subgroup-specific correlation using ANOVA and data presented in box plots. Log-rank analysis was performed using the Kaplan–Meier method to determine statistical difference of survival significance in the tumor xenograft studies. The number of samples used and the respective *P* values are listed in the figure legends. Significance for *in vitro* cell growth/death data was determined by Student two-tailed *t* test (N.S., not significant; *, $P < 0.05$; **, $P < 0.01$).

Results

JPO2 induces metastatic and infiltrative medulloblastoma tumor growth *in vivo*

We previously observed that JPO2 promotes medulloblastoma transformation *in vitro*; however, the *in vivo* oncogenic potential of JPO2 has not yet been investigated. We therefore examined the effect of ectopic JPO2 expression on UW228 and DAOY medulloblastoma cells using orthotopic xenograft assays in nude mice. Strikingly, while mice injected with parental UW228-control cell lines exhibited no tumor growth even up to 60 days postinjection, 80% (8/10) of the mice injected with UW228-JPO2 cells developed rapidly growing, infiltrative cerebellar tumors. All mice (10/10) injected with stable DAOY-JPO2 cell lines also developed highly infiltrative cerebellar tumors whereas only 50% (6/12) of the mice injected with DAOY-control lines exhibited limited localized tumor growth (Fig. 1A). Xenografts from both UW228-JPO2 and DAOY-JPO2 cells exhibited anaplastic cellular features resembling the large cell/anaplastic histology of aggressive group 3 human medulloblastoma. Ki-67 stains confirmed that both UW228-JPO2 and DAOY-JPO2 xenografts infiltrated adjacent normal cerebellum with a particularly invasive growth pattern noted in DAOY-JPO2 tumors (Fig. 1B). Mice injected with UW228-JPO2 and DAOY-JPO2 exhibited significantly shortened survival (mean survival of 42 days; $P < 0.001$), as compared with mice with control cell injections (Fig. 1C). Notably, xenografts with JPO2 expression exhibited a higher frequency of metastases, spinal metastases were detected in 62.5% (5/8) of UW228-JPO2 and 70% (7/10) of DAOY-JPO2 tumor-bearing mice, as compared with only 8.3% (1/12) of mice with control DAOY xenografts ($P = 0.03$, Fig. 1D). These data indicate that like Myc, JPO2 is a potent oncogenic driver that can also directly induce aggressive and metastatic phenotypes in medulloblastoma.

JPO2 and LEDGF/p75 are coordinately upregulated and physically associated in medulloblastoma

To investigate mechanisms of JPO2 oncogenic signaling, we used mass spectrometry analyses to identify other binding partners of JPO2. These experiments revealed a spectrum of candidate JPO2 interactors with tumor-promoting and cell survival functions including LEDGF/p75, an HIV-integrase and known oncogenic protein (29–31), which has not been implicated in medulloblastoma to date. Transient transfection and coimmunoprecipitation assays (Fig. 2A) corroborated prior reported observations of JPO2 and LEDGF/p75 interaction in 293TV cells (32, 33). Significantly, coimmunoprecipitation experiments also revealed JPO2 binds to endogenous LEDGF/p75 in UW228-JPO2 medulloblastoma cells (Fig. 2B). These observations were further confirmed by immunofluorescence and confocal microscopy studies, which indicated nuclear colocalization of JPO2 and LEDGF/p75 in UW228-JPO2 as well as ONS76 medulloblastoma cells, which have high endogenous JPO2 expression (Fig. 2C).

To evaluate the significance of JPO2:LEDGF/p75 interaction in medulloblastoma, we examined gene expression patterns of both loci in publicly available human and mouse medulloblastoma expression datasets. Interestingly, these analyses showed *JPO2/jpo2* and *LEDGF/p75/ledgf/p75* were concordantly expressed at high levels across all medulloblastoma subtypes and in a spectrum of murine medulloblastoma models (Fig. 3A and B). Western blot analyses also showed frequent high coexpression of LEDGF/p75 and JPO2 in a majority of human medulloblastoma cell lines examined (Fig. 3C).

JPO2 and LEDGF/p75 specifically promotes medulloblastoma cell migration/invasion

To determine how JPO2 and LEDGF/p75 may act together to promote medulloblastoma transformation, we examined the cellular effects of JPO2 and LEDGF/p75 expression in medulloblastoma cells. In contrast to Myc, BrdUrd, MTS, and cell count assays revealed that neither ectopic expression of JPO2 (Supplementary Fig. S1A–S1C) nor *JPO2* knockdown (Supplementary Fig. S1D and S1E) altered cell growth or proliferation across several different medulloblastoma cell lines. JPO2 expression also had little effect on medulloblastoma cell survival when cells were grown under conditions of serum starvation or exposed to radiation and various chemotherapeutic agents (Supplementary Fig. S2A–S2C). Consistent with its known function as a prosurvival protein, LEDGF/p75 expression enhanced survival of medulloblastoma cells exposed to serum starvation or chemotherapeutic drugs (Supplementary Fig. S3A) but had insignificant effects on medulloblastoma cell growth under normal proliferative conditions (Supplementary Fig. S3B).

As Myc and JPO2 are associated with metastatic medulloblastoma (5, 11), we examined whether JPO2 or LEDGF/p75 expression altered migratory and invasive phenotypes in medulloblastoma. Expression of JPO2 and LEDGF/p75 individually significantly enhanced medulloblastoma cell migration and invasion in Boyden chamber assays. Specifically, UW228, UW426, and DAOY cell lines with stable JPO2 or LEDGF/p75 expression showed 2- to 5-fold greater cell migration/invasion as compared with control cell lines ($P < 0.01$; Fig. 4A and B). Conversely, siRNA-mediated knockdown of *JPO2* or *LEDGF/p75* in medulloblastoma cell lines ONS76, D341, and D458, which express high endogenous levels of both proteins, diminished medulloblastoma cell migration and invasion by more than 50% (Fig. 4C and D).

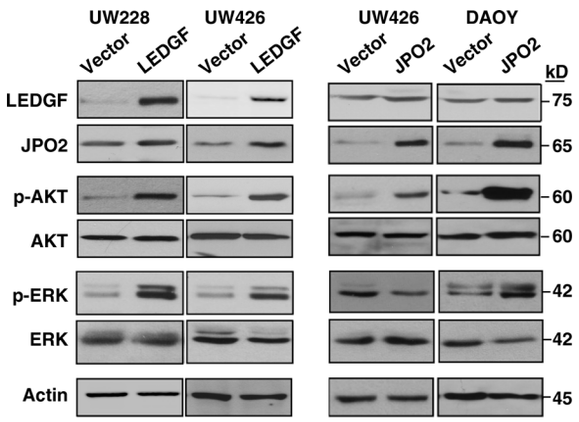

Figure 5.
LEDGF/p75 and JPO2 converge on PI3K/AKT signaling. Western blot analyses of JPO2, LEDGF, phospho AKT-T308, total AKT, phospho-, and total ERK1/2 expression in UW228-LEDGF, UW426-LEDGF, UW426-JPO2, DAOY-JPO2, and control cell lines; actin served as loading control.

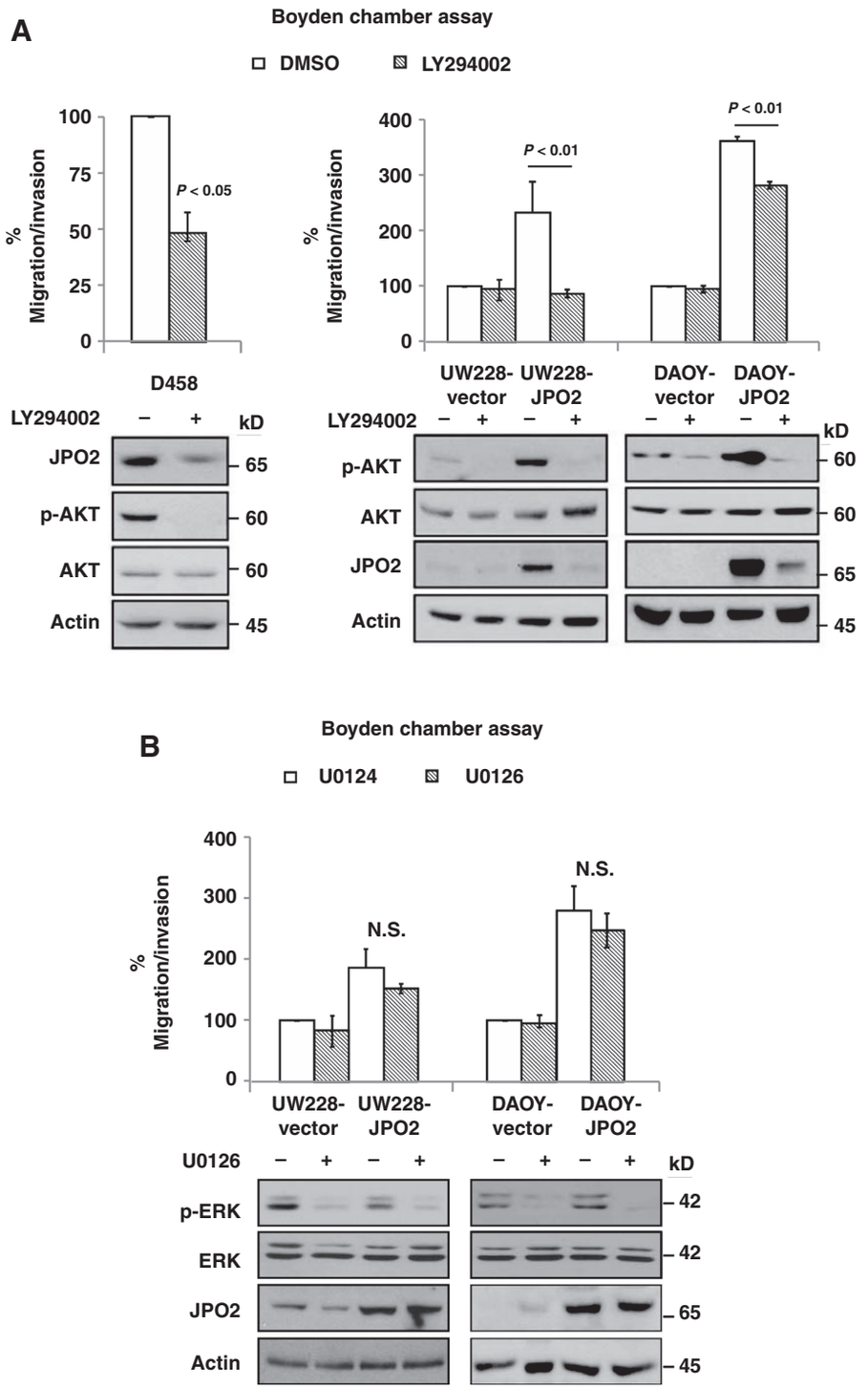

Figure 6.
JPO2-dependent medulloblastoma migration is AKT dependent. Medulloblastoma cells were pretreated with DMSO or 10 nmol/L LY294002 (3 hours; A) or 10 nmol/L U0126 (MEK1/2 inhibitor) or U0124 (control inactive analogue; 1 hour; B), then seeded (3.5×10^4 cells) in Boyden chambers and migrated cells were determined by direct cell count after 22 to 48 hours. Percent cell migration determined relative to controls is summarized for $n = 3$ experiments with 2 replicas/data point and is shown with corresponding Western blots confirming inhibition of AKT or ERK1/2 phosphorylation. Error bars, SEM; *, $P < 0.05$; **, $P < 0.01$. N.S., nonsignificant.

To further investigate whether medulloblastoma cell migration was functionally linked to JPO2 and LEDGF/p75 interaction, we performed siRNA-mediated knockdown of *JPO2* and *LEDGF/p75*, respectively, in medulloblastoma cells with LEDGF/p75 or JPO2 overexpression. Significantly, migration of UW228-JPO2 cells with *LEDGF/p75* knockdown and UW228-LEDGF cells with *JPO2* knockdown were, respectively, diminished by 35% and 50% relative to controls (Fig. 4E). Interestingly, corresponding qRT-PCR and Western blot analyses showed that *JPO2* mRNA and protein expression were also diminished with *LEDGF/p75* knockdown in UW228-JPO2 (Fig. 4E and F) and ONS76 cells (Supplementary Fig. S4A) and conversely, *JPO2* mRNA was upregulated in medulloblastoma cells with stable LEDGF/p75 expression (Supplementary Fig.

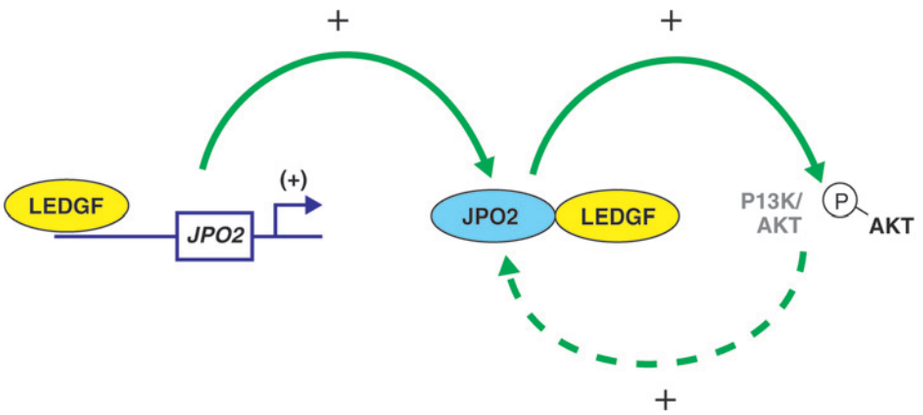

Figure 7.
Multiple feed-forward circuits link JPO2:LEDGF/p75:AKT to drive prometastatic signaling in medulloblastoma.

S4B). In contrast, LEDGF/p75 mRNA and protein expression remained unchanged with JPO2 overexpression or knockdown (Figs. 4E and 5 and Supplementary Fig. S4C). These findings suggest LEDGF/p75 and JPO2 may act via a feed-forward regulatory loop to modulate a common signaling axis and promote medulloblastoma cell migration/invasion.

LEDGF/p75 and JPO2 converge on PI3K/AKT signaling to drive medulloblastoma cell migration

To further elucidate mechanisms underlying the promigratory effects of JPO2 and LEDGF/p75 in medulloblastoma cells, we investigated effects of ectopic JPO2 and LEDGF/p75 expression on signaling pathways that have been implicated in medulloblastoma migration/metastases including PI3K/AKT and mitogen-associated protein kinase ERK1/2 pathways (13, 34–36). Interestingly, Western blot analyses of medulloblastoma cell lines with ectopic or endogenous LEDGF/p75 expression showed that LEDGF/p75 expression was accompanied by increased phospho-AKT-T308 as well as JPO2 expression (Fig. 5 and Supplementary Fig. S5). Similarly, ectopic JPO2 expression correlated with increased phospho-AKT-T308 levels. In contrast, we did not observe a consistent correlation of JPO2 expression with phospho-ERK1/2 signaling in different medulloblastoma cell lines, whereas LEDGF/p75 expression was associated with increased phospho-ERK1/2 level. These findings indicate that medulloblastoma cell migration and invasion is mediated by convergence of LEDGF/p75 and JPO2 on AKT.

To confirm the specific role of JPO2:AKT signaling in medulloblastoma cell migration, we examined the effect of PI3K inhibitor, LY294002, which blocks AKT phosphorylation, on migration of medulloblastoma cell lines with high endogenous (D458) and exogenous JPO2 expression (UW228-JPO2; DAOY-JPO2). Treatment with LY294002 inhibited D458 cell migration and reversed the promigratory effects of exogenous JPO2 expression in UW228 and DAOY cell lines (Fig. 6A). However in contrast to UW228-Myc cells, survival of UW228-JPO2 cells was not altered by LY294002 treatment (Supplementary Fig. S6A and S6B). Importantly, the inhibitory effect of LY294002 treatment on JPO2-induced cell migration was highly specific as treatment with MEK1/2 inhibitor, U0126, which blocks ERK1/2 phosphorylation, as well as a control inactive analog, U0124, had no effects UW228-JPO2 and DAOY-JPO2 cell migration (Fig. 6B). In keeping with the specific association of JPO2-induced cell migration with the AKT pathway, we observed a decrease in phospho-AKT expression in all 3 medulloblastoma cell lines with inhibition of cell migration. Interestingly, this was also accompanied by a decrease in JPO2 protein (Fig. 6A) but not mRNA expression (Supplementary Fig. S7), thus indicating posttranslational regulation of JPO2 by AKT.

Our collective experimental studies support a model in which the prometastatic functions of AKT signaling are dependent and promoted by two novel and synergistic feed-forward regulatory circuits between LEDGF/p75 and JPO2 and between JPO2 and AKT (Fig. 7). These findings highlight JPO2 and LEDGF/p75 as new and important avenues for targeting the prometastatic AKT signaling cascade in medulloblastoma.

Discussion

Substantial data implicate Myc and PI3K activation in aggressive phenotypes and treatment resistance in medulloblastoma (5, 7, 15, 19, 20, 37–39). To date, multiple studies have demonstrated that pharmacologic inhibitors of PI3K signaling have potent antineoplastic effects in medulloblastoma (7, 13, 14, 16, 17, 19, 36), and underscore the importance of PI3K signaling particularly in Myc-driven medulloblastoma. To effectively exploit PI3K/AKT signaling for medulloblastoma treatment, it would be important to delineate the extent of the Myc–PI3K/AKT signaling axis through identification of novel targetable effector and mediators of this pathway. In this study, we identified JPO2 and LEDGF/p75 as novel components of PI3K/AKT signaling, and have uncovered complex new signaling circuits driven by JPO2 and LEDGF/p75, which promote migratory and invasive phenotypes in medulloblastoma via upregulation of PI3K/AKT signaling.

Our *in vitro* and *in vivo* studies indicate JPO2 specifically promotes medulloblastoma cell migration/invasion and metastases without effects on cell proliferation or survival. Although our observations strongly support a role for the JPO2:AKT axis on medulloblastoma cell migration, gross morphologic changes were not evident in medulloblastoma cells with JPO2 overexpression. Interestingly, we observed in preliminary studies that N-cadherin expression is diminished in medulloblastoma cells with ectopic JPO2 expression, thus suggesting JPO2 may mediate medulloblastoma migratory phenotypes in part by promoting epithelial–mesenchymal transition (EMT). Future studies to determine how JPO2 and the PI3K/AKT pathway act convergently or independently to mediate EMT and migratory/metastatic medulloblastoma phenotypes would clearly be of therapeutic interest.

We observed that JPO2 binds to LEDGF/p75, a known oncoprotein highly expressed in multiple cancer types (31, 40, 41), that is also coordinately upregulated with JPO2 in medulloblastoma. Our data, which is the first to implicate LEDGF/p75 in medulloblastoma suggest LEDGF/p75 and JPO2 may act via a common transcriptional signaling complex to promote Myc:PI3K/AKT-associated medulloblastoma transformation. Our observations that LEDGF/p75 regulates and functions cooperatively with JPO2 to promote prometastatic AKT signaling in medulloblastoma cells are concordant with reported LEDGF/p75 and JPO2 interactions in HEK 293 cells (32). We observed changes in JPO2 mRNA and protein levels with LEDGF/p75 expression in medulloblastoma cells that suggest transcriptional regulation of *JPO2* by LEDGF/p75. However, while we observed a significant overall upregulation of both genes in primary human and murine medulloblastoma, detailed *in silico* analyses of individual human medulloblastoma subtypes revealed a positive, but nonsignificant trend between *JPO2* and *LEDGF/p75* expression only in human SHH and group 3 medulloblastoma (Supplementary Fig. S8). Interestingly, studies by Bartholoomeeusen and colleagues (32) in HEK 293 cells demonstrate LEDGF/p75 also regulates JPO2 protein stability. These aggregate data suggest that LEDGF/p75 may regulate JPO2 via transcriptional as well as posttranscriptional mechanisms in a cell context–dependent manner. In addition to direct transcriptional functions, both LEDGF/p75 and JPO2 (42, 43) have been implicated in chromatin remodelling (44–46), thus JPO2:LEDGF/p75 transcriptional complexes may have more potent, global gene regulatory roles with impact on additional as yet undefined transforming pathways in medulloblastoma. Interestingly, recent studies also suggest potential E3 ubiquitin ligase functions for JPO2 (44, 47), thus JPO2 may also regulate signaling via posttranslational mechanisms. Future biochemical studies of JPO2 and JPO2:LEDGF/p75 interactions will be important for defining critical domains required for JPO2 and LEDGF/p75 cooperation in oncogenic signaling that may be exploited therapeutically.

LEDGF/p75 is a potent oncogene with known diverse functions in cell survival, chemotherapy resistance, tumor progression (41, 48, 49), and leukemic transformation via interactions with MLL oncoproteins (30). Although our studies indicated a tight convergence of LEDGF/p75 and JPO2 on promigratory AKT signaling, we observed that JPO2 and LEDGF/p75 did not always have overlapping cellular and signaling effects in UW228 and UW426 medulloblastoma cell lines. Specifically, while we observed inconsistent effects of JPO2 expression on p-ERK1/2 levels in UW228 and UW426 cells, ERK1/2 was consistently upregulated with LEDGF/p75 expression in the same cell lines (Fig. 5). Although effects of cell context remains to be examined with a wider panel of medulloblastoma cell lines, it is interesting to note that while pERK1/2 expression did not correlate with promigratory effects of LEDGF/p75 on medulloblastoma cells, each of the UW228, UW426, and DAOY cells examined exhibited enhanced survival with LEDGF/p75 expression (Supplementary Fig. S3A). Our collective observations support LEDGF/p75 as a novel and important driver of prometastatic phenotypes in medulloblastoma and indicate additional distinct oncogenic roles for LEDGF/p75 in medulloblastoma. Whether LEDGF/p75 can recapitulate the potent *in vivo* oncogenic and metastatic effects of Myc and JPO2 on medulloblastoma cells remains to be investigated. The relatively high expression of LEDGF/p75 and JPO2 in various human medulloblastoma subgroups and murine medulloblastoma models also suggest broader roles for LEDGF/p75 and/or JPO2 in medulloblastoma pathogenesis. Given the high expression of JPO2 expression in Myc as well as N-Myc–associated medulloblastoma, we anticipate JPO2 and LEDGF to also have roles in N-myc–driven PI3K signaling seen in the SHH subtype of medulloblastoma (50, 51).

In summary, we have discovered a new and complex signaling circuit that promotes prometastatic activity of the PI3K/AKT pathway in medulloblastoma. Our data implicates two oncoproteins JPO2 and LEDGF/p75 as novel modulators of PI3K/AKT signaling and suggest potential new avenues for targeting the potent Myc:PI3K/AKT signaling axis, which underlies the most lethal phenotypes in medulloblastoma.

Disclosure of Potential Conflicts of Interest

No potential conflicts of interest were disclosed.

Authors' Contributions

Conception and design: T.S.Y. Chan, C.J. McGlade, A. Huang
Development of methodology: T.S.Y. Chan, C.J. McGlade, A. Huang
Acquisition of data (provided animals, acquired and managed patients, provided facilities, etc.): T.S.Y. Chan, C. Hawkins, J.R. Krieger, A. Huang
Analysis and interpretation of data (e.g., statistical analysis, biostatistics, computational analysis): T.S.Y. Chan, C. Hawkins, J.R. Krieger, A. Huang
Writing, review, and/or revision of the manuscript: T.S.Y. Chan, A. Huang
Administrative, technical, or material support (i.e., reporting or organizing data, constructing databases): A. Huang
Study supervision: A. Huang

Acknowledgments

The authors thank L. Penn for Myc antibodies and D. Picard for technical help in generating JPO2 stably expressing cell lines.

Grant Support

This work was supported by Canadian Institute of Health Research grant #MOP-119591. T.S.Y. Chan received a University of Toronto Fellowship, Frank Fletch Memorial Research Fund, and Clayton Pediatric Research Fund.

The costs of publication of this article were defrayed in part by the payment of page charges. This article must therefore be hereby marked *advertisement* in accordance with 18 U.S.C. Section 1734 solely to indicate this fact.

Received August 13, 2015; revised February 1, 2016; accepted February 26, 2016; published OnlineFirst March 24, 2016.

References

1. Mazzola CA, Pollack IF.Medulloblastoma. Curr Treat Options Neurol 2003;5:189–98.
2. Packer RJ, Vezina G.Management of and prognosis with medulloblastoma: therapy at a crossroads.Arch Neurol 2008;65:1419–24.
3. Northcott PA, Korshunov A, Pfister SM, Taylor MD. The clinical implications of medulloblastoma subgroups. Nat Rev Neurol 2012; 8:340–51.
4. Ellison DW, Dalton J, Kocak M, Nicholson SL, Fraga C, Neale G, et al. Medulloblastoma: clinicopathological correlates of SHH, WNT, and non-SHH/WNT molecular subgroups. Acta Neuropathol 2011; 121:381–96.
5. Taylor MD, Northcott PA, Korshunov A, Remke M, Cho YJ, Clifford SC, et al. Molecular subgroups of medulloblastoma: the current consensus. Acta Neuropathol 2012;123:465–72.

6. Zhou L, Picard D, Ra YS, Li M, Northcott PA, Hu Y, et al. Silencing of thrombospondin-1 is critical for myc-induced metastatic phenotypes in medulloblastoma. Cancer Res 2010;70:8199–210.
7. Pei Y, Moore CE, Wang J, Tewari AK, Eroshkin A, Cho YJ, et al. An animal model of MYC-driven medulloblastoma. Cancer Cell 2012; 21:155–67.
8. Ryan SL, Schwalbe EC, Cole M, Lu Y, Lusher ME, Megahed H, et al. MYC family amplification and clinical risk-factors interact to predict an extremely poor prognosis in childhood medulloblastoma. Acta Neuropathol 2012;123:501–13.
9. Wright KD, von der Embse K, Coleman J, Patay Z, Ellison DW, Gajjar A. Isochromosome 17q, MYC amplification and large cell/anaplastic phenotype in a case of medullomyoblastoma with extracranial metastases. Pediatr Blood Cancer 2012;59:561–4.
10. Roussel MF, Robinson GW. Role of MYC in medulloblastoma. Cold Spring Harb Perspect Med 2013;3.
11. Kawauchi D, Robinson G, Uziel T, Gibson P, Rehg J, Gao C, et al. A mouse model of the most aggressive subgroup of human medulloblastoma. Cancer Cell 2012;21:168–80.
12. Dijkgraaf GJ, Alicke B, Weinmann L, Januario T, West K, Modrusan Z, et al. Small molecule inhibition of GDC-0449 refractory smoothened mutants and downstream mechanisms of drug resistance. Cancer Res 2011;71:435–44.
13. Ehrhardt M, Craveiro RB, Holst MI, Pietsch T, Dilloo D. The PI3K inhibitor GDC-0941 displays promising *in vitro* and *in vivo* efficacy for targeted medulloblastoma therapy. Oncotarget 2015;6:802–13.
14. Guerreiro AS, Fattet S, Fischer B, Shalaby T, Jackson SP, Schoenwaelder SM, et al. Targeting the PI3K p110alpha isoform inhibits medulloblastoma proliferation, chemoresistance, and migration. Clin Cancer Res 2008; 14:6761–9.
15. Metcalfe C, Alicke B, Crow A, Lamoureux M, Dijkgraaf GJ, Peale F, et al. PTEN loss mitigates the response of medulloblastoma to Hedgehog pathway inhibition. Cancer Res 2013;73:7034–42.
16. Salm F, Dimitrova V, von Bueren A O, C´wiek P, Rehrauer H, Djonov V, et al. The Phosphoinositide 3-Kinase p110alpha isoform regulates leukemia inhibitory factor receptor expression via c-Myc and miR-125b to promote cell proliferation in medulloblastoma. PLoS One 2015;10:e0123958.
17. Guerreiro AS, Fattet S, Kulesza DW, Atamer A, Elsing AN, Shalaby T, et al. A sensitized RNA interference screen identifies a novel role for the PI3K p110gamma isoform in medulloblastoma cell proliferation and chemoresistance. Mol Cancer Res 2011;9:925–35.
18. Hartmann W, Digon-Söntgerath B, Koch A, Waha A, Endl E, Dani I, et al. Phosphatidylinositol 3′-kinase/AKT signaling is activated in medulloblastoma cell proliferation and is associated with reduced expression of PTEN. Clin Cancer Res 2006;12:3019–27.
19. Baryawno N, Sveinbjörnsson B, Eksborg S, Chen CS, Kogner P, Johnsen JI. Small-molecule inhibitors of phosphatidylinositol 3-kinase/Akt signaling inhibit Wnt/beta-catenin pathway cross-talk and suppress medulloblastoma growth. Cancer Res 2010;70: 266–76.
20. Wu X, Northcott PA, Dubuc A, Dupuy AJ, Shih DJ, Witt H, et al. Clonal selection drives genetic divergence of metastatic medulloblastoma. Nature 2012;482:529–33.
21. Mumert M, Dubuc A, Wu X, Northcott PA, Chin SS, Pedone CA, et al. Functional genomics identifies drivers of medulloblastoma dissemination. Cancer Res 2012;72:4944–53.
22. Aref D, Croul S. Medulloblastoma: recurrence and metastasis. CNS Oncol 2013;2:377–85.
23. Huang A, Ho CS, Ponzielli R, Barsyte-Lovejoy D, Bouffet E, Picard D, et al. Identification of a novel c-Myc protein interactor, JPO2, with transforming activity in medulloblastoma cells. Cancer Res 2005; 65:5607–19.
24. Lee Y, Miller HL, Jensen P, Hernan R, Connelly M, Wetmore C, et al. A molecular fingerprint for medulloblastoma. Cancer Res 2003;63: 5428–37.
25. Prescott JE, Osthus RC, Lee LA, Lewis BC, Shim H, Barrett JF, et al. A novel c-Myc-responsive gene, JPO1, participates in neoplastic transformation. J Biol Chem 2001;276:48276–84.
26. Osthus RC, Karim B, Prescott JE, Smith BD, McDevitt M, Huso DL, et al. The Myc target gene JPO1/CDCA7 is frequently overexpressed in human tumors and has limited transforming activity *in vivo*. Cancer Res 2005;65:5620–7.
27. Dennis-Sykes CA, Miller WJ, McAleer WJ. A quantitative Western Blot method for protein measurement. J Biol Stand 1985;13:309–14.
28. Northcott PA, Shih DJ, Peacock J, Garzia L, Morrissy AS, Zichner T, et al. Subgroup-specific structural variation across 1,000 medulloblastoma genomes. Nature 2012;488:49–56.
29. Llano M, Saenz DT, Meehan A, Wongthida P, Peretz M, Walker WH, et al. An essential role for LEDGF/p75 in HIV integration. Science 2006;314:461–4.
30. Yokoyama A, Cleary MLMenin critically links MLL proteins with LEDGF on cancer-associated target genes. Cancer Cell 2008;14:36–46.
31. Grand FH, Koduru P, Cross NC, Allen SL. NUP98-LEDGF fusion and t(9;11) in transformed chronic myeloid leukemia. Leuk Res 2005; 29:1469–72.
32. Bartholomeeusen K, De Rijck J, Busschots K, Desender L, Gijsbers R, Emiliani S, et al. Differential interaction of HIV-1 integrase and JPO2 with the C terminus of LEDGF/p75. J Mol Biol 2007;372:407–21.
33. Maertens GN, Cherepanov P, Engelman A. Transcriptional co-activator p75 binds and tethers the Myc-interacting protein JPO2 to chromatin. J Cell Sci 2006;119:2563–71.
34. Parri M, Chiarugi P. Rac and Rho GTPases in cancer cell motility control. Cell Commun Signal 2010;8:23.
35. Wøodarski P, Grajkowska W, èojek M, Rainko K, Jóźwiak J. Activation of Akt and Erk pathways in medulloblastoma. Folia Neuropathol 2006; 44:214–20.
36. Wojtalla A, Salm F, Christiansen DG, Cremona T, Cwiek P, Shalaby T, et al. Novel agents targeting the IGF-1R/PI3K pathway impair cell proliferation and survival in subsets of medulloblastoma and neuroblastoma. PLoS One 2012;7:e47109.
37. Aldosari N, Bigner SH, Burger PC, Becker L, Kepner JL, Friedman HS, et al. MYCC and MYCN oncogene amplification in medulloblastoma. A fluorescence *in situ* hybridization study on paraffin sections from the Children's Oncology Group. Arch Pathol Lab Med 2002;126:540–4.
38. Eberhart CG, Kratz J, Wang Y, Summers K, Stearns D, Cohen K, et al. Histopathological and molecular prognostic markers in medulloblastoma: c-myc, N-myc, TrkC, and anaplasia. J Neuropathol Exp Neurol 2004;63: 441–9.
39. Bandopadhayay P, Bergthold G, Nguyen B, Schubert S, Gholamin S, Tang Y, et al. BET bromodomain inhibition of MYC-amplified medulloblastoma. Clin Cancer Res 2014;20:912–25.
40. Bhargavan B, Fatma N, Chhunchha B, Singh V, Kubo E, Singh DP. LEDGF gene silencing impairs the tumorigenicity of prostate cancer DU145 cells by abating the expression of Hsp27 and activation of the Akt/ERK signaling pathway. Cell Death Dis 2012;3:e316.
41. Huang TS, Myklebust LM, Kjarland E, Gjertsen BT, Pendino F, Bruserud Ø, et al. LEDGF/p75 has increased expression in blasts from chemotherapy-resistant human acute myelogenic leukemia patients and protects leukemia cells from apoptosis *in vitro*. Mol Cancer 2007;6:31.
42. Chen K, Ou XM, Wu JB, Shih JC. Transcription factor E2F-associated phosphoprotein (EAPP), RAM2/CDCA7L/JPO2 (R1), and simian virus 40 promoter factor 1 (Sp1) cooperatively regulate glucocorticoid activation of monoamine oxidase B. Mol Pharmacol 2011;79:308–17.
43. Rivera-Gonzalez GC, Droop AP, Rippon HJ, Tiemann K, Pellacani D, Georgopoulos LJ, et al. Retinoic acid and androgen receptors combine to achieve tissue specific control of human prostatic transglutaminase expression: a novel regulatory network with broader significance. Nucleic Acids Res 2012;40:4825–40.
44. Yang L, Lin C, Liu W, Zhang J, Ohgi KA, Grinstein JD, et al. ncRNA- and Pc2 methylation-dependent gene relocation between nuclear structures mediates gene activation programs. Cell 2011;147:773–88.
45. Pfister SX, Ahrabi S, Zalmas LP, Sarkar S, Aymard F, Bachrati CZ, et al. SETD2-dependent histone H3K36 trimethylation is required for homologous recombination repair and genome stability. Cell Rep 2014;7:2006–18.
46. Daugaard M, Baude A, Fugger K, Povlsen LK, Beck H, Sørensen CS, et al. LEDGF (p75) promotes DNA-end resection and homologous recombination. Nat Struct Mol Biol 2012;19:803–10.
47. Rigbolt KT, Prokhorova TA, Akimov V, Henningsen J, Johansen PT, Kratchmarova I, et al. System-wide temporal characterization of the proteome and phosphoproteome of human embryonic stem cell differentiation. Sci Signal 2011;4:rs3.

48. Daugaard M, Kirkegaard-Sørensen T, Ostenfeld MS, Aaboe M, Høyer-Hansen M, Orntoft TF, et al. Lens epithelium-derived growth factor is an Hsp70–2 regulated guardian of lysosomal stability in human cancer. Cancer Res 2007;67:2559–67.
49. Brown-Bryan TA, Leoh LS, Ganapathy V, Pacheco FJ, Mediavilla-Varela M, Filippova M, et al. Alternative splicing and caspase-mediated cleavage generate antagonistic variants of the stress oncoprotein LEDGF/p75. Mol Cancer Res 2008;6:1293–307.
50. Browd SR, Kenney AM, Gottfried ON, Yoon JW, Walterhouse D, Pedone CA, et al. N-myc can substitute for insulin-like growth factor signaling in a mouse model of sonic hedgehog-induced medulloblastoma. Cancer Res 2006;66:2666–72.
51. Rao G, Pedone CA, Del Valle L, Reiss K, Holland EC, Fults DW. Sonic hedgehog and insulin-like growth factor signaling synergize to induce medulloblastoma formation from nestin-expressing neural progenitors in mice. Oncogene 2004;23:6156–62.